Therapeutic Efficacy of Large Aligned Cardiac Tissue Derived from Induced Pluripotent Stem Cell in a Porcine Ischemic Cardiomyopathy Model

Kota Suzuki MD , Shigeru Miyagawa MD, PhD , Li Liu MD, PhD , Takuji Kawamura MD, PhD , Junjun Li PhD , Xiang Qu MD , Akima Harada BSC , Koichi Toda MD, PhD , Daisuke Yoshioka MD, PhD , Satoshi Kainuma MD, PhD , Ai Kawamura MD, PhD , Yoshiki Sawa MD, PhD

PII: S1053-2498(21)02282-8
DOI: https://doi.org/10.1016/j.healun.2021.04.010
Reference: HEALUN 7385

To appear in: *Journal of Heart and Lung Transplantation*

Please cite this article as: Kota Suzuki MD , Shigeru Miyagawa MD, PhD , Li Liu MD, PhD , Takuji Kawamura MD, PhD , Junjun Li PhD , Xiang Qu MD , Akima Harada BSC , Koichi Toda MD, PhD , Daisuke Yoshioka MD, PhD , Satoshi Kainuma MD, PhD , Ai Kawamura MD, PhD , Yoshiki Sawa MD, PhD , Therapeutic Efficacy of Large Aligned Cardiac Tissue Derived from Induced Pluripotent Stem Cell in a Porcine Ischemic Cardiomyopathy Model, *Journal of Heart and Lung Transplantation* (2021), doi: https://doi.org/10.1016/j.healun.2021.04.010

Title Page:

Therapeutic Efficacy of Large Aligned Cardiac Tissue Derived from Induced Pluripotent Stem Cell in a Porcine Ischemic Cardiomyopathy Model

Kota Suzuki, MD, [a] Shigeru Miyagawa, MD, PhD, [a] Li Liu, MD, PhD, [a] Takuji Kawamura MD, PhD, [a] Junjun Li, PhD, [a] Xiang Qu, MD, [a] Akima Harada BSC, [a] Koichi Toda MD, PhD, [a] Daisuke Yoshioka MD, PhD, [a] Satoshi Kainuma MD, PhD, [a] Ai Kawamura MD, PhD, [a] Yoshiki Sawa, MD, PhD [a]

Institutions:

[a] Department of Cardiovascular Surgery, Osaka University Graduate School of Medicine, Osaka, Japan

Corresponding Author: Yoshiki Sawa

[1] Department of Cardiovascular Surgery, Osaka University Graduate School of Medicine

2-2 Yamadaoka, Suita, Osaka 565-0871, Japan

Phone/Fax: +81-6-6879-3154

E-mail: sawa-p@surg1.med.osaka-u.ac.jp

Running title: Aligned cardiac tissue transplantation

Word Count: 2999 words

Nonstandard Abbreviations and Acronyms

iPS cell = induced pluripotent stem cell

iPS-CM = induced pluripotent stem cell-derived cardiomyocytes

PDMS = poly-dimethylsiloxane

FISH = fluorescent *in situ* hybridization

MEA = microelectrode array

GLS = global longitudinal strain

ABSTRACT

BACKGROUND:

Although induced pluripotent stem (iPS) cell-derived cardiac constructs may have a potential in cardiomyogenesis of a distressed myocardium, obtaining polarity in cardiac constructs, such as via myocyte alignment, may be crucial to achieve a maximum contractile force for better clinical outcomes. We herein hypothesized that transplantation of an aligned cardiac tissue derived from iPS cells has therapeutic effects in a porcine ischemic cardiomyopathy model as a preclinical trial.

METHODS:

Aligned cardiac tissues were developed by culturing high-purity iPS cell-derived cardiomyocytes in xeno-free conditions and transplanting them into infarct porcine hearts (iPS-CM group, n = 7; control, n = 6). Three months after treatment, therapeutic efficacy was evaluated functionally and histologically.

RESULTS:

In vitro assessment revealed that the aligned cardiac tissue containing high purity cardiomyocytes contracted homogeneously and had excellent mechanical properties. In the *in vivo* study, the left ventricular ejection fraction of the iPS-CM group was significantly greater than that of the control group, 3 months after transplantation (37.8% ± 2.3% versus 28.3% ± 2.5%, $p < 0.05$). Pathologically, attenuated interstitial fibrosis, attenuation of hypertrophied cardiomyocytes, and an increased capillary density were also prominent in the iPS-CM group. A limited amount of engraftment of the transplanted tissue maintaining tissue alignment was observed at 2 weeks after transplantation.

CONCLUSIONS:

The creation of large-scale functional aligned cardiac tissue was feasible, and the transplantation of the aligned tissue improved cardiac function with angiogenesis and antifibrotic effects in a porcine cardiomyopathy model.

(239 words)

Introduction

In the era of a pandemic situation of heart failure, regenerative therapy using induced pluripotent stem (iPS) cells may be one of options that potentially coexist alongside clinically restricted strategies, including heart transplantation and left ventricular assist device. [1,2] However, for the clinical application, several critical points must be clear, such as the manufacture cost with a stable production of cardiomyocytes and transplantation methodology.

Cardiomyocyte differentiation methods have a potential risk of infection due to the use of several ingredients that originate from human and animal sources, such as serum proteins and growth factors. [3–5] Moreover, it may be costly to prepare a large number of cardiomyocytes for transplantation into the human heart. To solve some of the drawbacks mentioned above, specific small molecules, such as KY02111, that can differentiate iPS cells into ventricular type cardiomyocytes with a low cost, have been developed.[6]

Another point is the effective methodology in transplantation that has the potential to ameliorate severe heart failure, in which few cardiomyocytes remain. The generation of a functional myocardial tissue is one option to propose "cardiomyogenesis." In particular, an important aspect of a functional cardiac tissue has to do with how to regulate the alignment of cardiomyocytes to achieve a more powerful contraction. It has been reported that cardiac tissue with cardiomyocyte alignment using nanofiber technology has the advantage of electrophysiology and cardiomyocyte maturation *in vitro*[7,8] with evidence of functional recovery after *in vivo* transplantation using a rat infarction model [7]. However, proof of concept using a large animal heart failure model as a preclinical study has not been revealed yet. The hypothesis of this study is that large-scale cardiac tissue with an aligned nanofiber scaffold could ameliorate the cardiac function in a porcine ischemic cardiomyopathy model.

Materials and methods

Cell Motion Analysis

The contractile properties were evaluated using a Cell Motion Imaging System (SI8000; SONY, Tokyo, Japan). Videos of aligned and non-aligned cardiac tissue were recorded at a frame rate of 150 frames per second, a resolution of 512 × 512 pixels, and a depth of 8 bits. We observed aligned and non-aligned cardiac tissues directly in a 6-well plate.

Animal Care

The experimental protocol was approved by the Animal Care Committee of the Osaka University Graduate School of Medicine. The animal care procedures used in this study complied with the Guide for the Care and Use of Laboratory Animals (National Institutes of Health publication No. 85-23, revised, 1996).

Ischemic Cardiomyopathy Model of Porcine

An ischemic cardiomyopathy model of porcine was generated using a previously reported method.[9] In brief, the experiments were performed using male Gottingen minipigs weighing 20–25 kg (Ellegaard, Dalmose, Denmark). The animals were anesthetized, endotracheally intubated, and mechanically ventilated. Anesthesia was maintained by inhalation of isoflurane (Wako Pure Chemical Industries). An ameroid ring constrictor (MRI-4.00-TI; Research Instruments NWInc, Lebanon, Ore) was attached to the proximal left anterior descending coronary artery via left thoracotomy. Standard postoperative care was carried out according to the Animal Use Guidelines of Osaka University.

Aligned Cardiac Tissue Transplantation

HiPSC-CMs (2.5×10^7 cells/sheet) were seeded on the aligned nanofiber in a 2.5 × 2.5 cm poly-dimethylsiloxane (PDMS) frame for 2 days. Four weeks after myocardial infarction

induction, the aligned cardiac tissue (4 sheets, 1×10^8 cardiomyocytes), or nanofiber scaffold without cardiomyocytes (Control) was transplanted into the infarct region of the heart and subsequently covered with pericardium by disseminating Beri-plast P (CSL Behring, USA) via median sternotomy. Because human cells were administered to porcine (xenotransplantation) in this experiment, the animals in both groups were administered three oral immunosuppressants (tacrolimus, 0.75 mg/kg per day; mycophenolate mofetil, 500 mg/day; corticosteroids, 20 mg/day).

Fluorescent *in situ* hybridization (FISH)

Two weeks after transplantation, hiPS-CMs were analyzed using fluorescent *in situ* hybridization (FISH) by using a human-specific genomic probe labeled as described previously[1]. Briefly, 3-mm-thick sections were deparaffinized, washed in phosphate-buffered saline for 5 min, digested in a pepsin solution (0.1% in 0.1 N HCl) at 37°C for 10 min, and dehydrated. A species-specific FISH human probe (Chromosome Science Labo Inc.) labeled with Cy3 was applied to the pretreated sections, covered with cover slips, and simultaneously denatured at 90°C for 10 min. Hybridization was carried out at 37°C overnight. Sections were then washed with 50% formamide 2x saline sodium citrate buffer (SSC) at 37°C for 20 min, 1xSSC at 24°C for 15 min, counterstained with 4, 6-diamidino-2phenylindole (DAPI), and mounted.

Statistical Analysis

Data were expressed as mean ± standard deviation and analyzed using JMP Pro 14 software (SAS Institute, Tokyo, Japan). Statistical significance was determined using Student's *t*-test (2-tailed) for comparisons between two groups. The values for different experimental conditions within a group were compared to the baseline using a paired *t-test*. Differences between more than three groups were evaluated by the one-way analysis of variance, and comparison of the time-course analysis was evaluated by 2-way repeated measures analysis of variance. When a significant effect was detected, we performed Tukey-Kramer post hoc analysis to determine significance for specific comparisons at each time point. $P < 0.05$ was considered statistically significant.

Results

Characterization of transplanted hiPS-derived cardiomyocytes in protein-free differentiation method

Cardiac differentiation of hiPS cells was induced using six small molecules (CHIR99021, PMA in the early phase, and KY03-I, XAV939, A419259, and AG1478 in the late phase) in peptide-free, protein-free conditions (Figure 1A). The ratio of cardiac troponin T (cTnT)-positive cardiomyocytes used in this differentiation method was 92.1% ± 1.9% (n = 8),

according to flow cytometry analysis (Figure 1B). Spontaneous contractions were observed on day 7 after differentiation was initiated (Movie S1). Because the protein-free medium we developed consists of only IMDM/DMEM medium and low molecular weight constituents (Table S1, S2), it is extremely cost-effective (approximately 4.59 US dollars per 2×10^7 cardiomyocytes). Regarding the type of cardiomyocytes, flow cytometry analysis revealed that the ratios of myosin light chain 2v (MLC2v) single-positive (relatively mature ventricular) cells, MLC2a single-positive (atrial) cells, and hyperpolarization activated cyclic nucleotide gated potassium channel 4 (HCN4)-positive (pacemaker) cells were 70.5% ± 3.4%, 0.2% ± 0.1%, and 10.3% ± 1.7%, respectively (n = 4). On the other hand, the MLC2v/MLC2a double-positive (relatively immature ventricular cells) cell ratio was 8.6% ± 2.0% (Figure 1C, 1D). These data indicated that this differentiation method produced a relatively high percentage of mature ventricular type cardiomyocytes. Fluorescence immunostaining revealed that the iPS-derived cardiomyocytes expressed cTnT and alpha sarcomeric actinin (Figure 1E), which indicated a well-arranged, clear sarcomeric structure.

Characterization of large-scale aligned cardiac tissue

The nanofibers were fabricated in the same way as in our previous report. The nanofibers were transferred to a large PDMS frame (2.5×2.5 cm^2, Figure 2A, 2B). Large-scale aligned cardiac tissue was fabricated by simply seeding 25 million iPS-derived cardiomyocytes onto the fiber

sheet. The thickness of this cardiac tissue was approximately 100 – 150 μm, as illustrated by hematoxylin and eosin staining results (Figure 2C). Scanning electron microscopy images revealed that the cardiomyocytes were aligned along the nanofiber scaffold (Figure 2D, 2E). After 2 weeks of culture, immunostaining for cardiac tissue-specific markers revealed that cTnT-positive myofilaments and α-actinin-positive sarcomeres were well defined and positioned along the nanofiber scaffold (Figure 2F). In addition, cardiac gap junction protein connexin 43 (Figure 2G) and cardiac maturation markers related to contractile velocity (β-myosin heavy chain [Figure 2H]) were highly expressed, suggesting structural and electrophysiological maturation.

Electrophysiology and contractile properties of aligned cardiac tissue

Electrophysiology of large-scale aligned cardiac tissue was recorded using a microelectrode array (MEA) system (Figure 3A). The activation map indicated a homogeneous propagation of the electrical signal, and no conduction delay was found, confirming the organization and synchronization of cardiomyocytes (Figure 3B). In addition, the velocity of transmission in the transverse direction (along the direction of the nanofiber) was higher than the velocity of transmission in the longitudinal direction (not along the direction of the nanofiber), which indicated the anisotropic propagation of this aligned cardiac tissue. The field potential could be recorded in all 59 channels on the MEA (Figure 3C). These findings indicated that

large-scale cardiac tissue showed a homogeneous contractility and an anisotropic propagation, similar to the small aligned cardiac tissue (1 cm × 1 cm). The calcium handling test revealed that aligned cardiac tissue responded to the addition of 5 mM caffeine, as significantly higher peak intensity was observed. Quantification of the calcium transient showed an 11 ± 7.6% (n=3) change in peak intensity, suggesting the functional maturation of the cardiac tissue (Figure 3D). We also measured cytokine concentrations in the culture supernatant to investigate the angiogenic effect, which showed cytokine release related to angiogenesis, including VEGF and SDF-1 (Figure S1A, S1B). Furthermore, in order to prove the superiority of the aligned cardiac tissue regarding its mechanical properties, we evaluated the contractility of the aligned and non-aligned cardiac tissue using the Cell Motion Imaging System (Figure 3E, Movie S2-S5). Aligned cardiac tissue showed a significantly higher acceleration (894 ± 211 vs. 536 ± 126 $\mu m/s^2$; $p = 0.009$), contraction velocity (30.1 ± 5.2 vs. 13.9 ± 4.1 μm/s; $p < 0.001$), and relaxation velocity (15.4 ± 3.1 vs. 8.0 ± 2.1 μm/s; $p = 0.001$) than the non-aligned cardiac tissue (Figure 3E-3G). The aligned cardiac tissue demonstrated improved contractile properties compared with the non-aligned cardiac tissue.

Transplantation of the aligned cardiac tissue ameliorates global and regional cardiac function after myocardial infarction

Cardiac function was evaluated using echocardiography every month and cardiac magnetic resonance imaging (CMR) before and 3 months after transplantation. Echocardiography revealed that the iPS-CM group showed a significant improvement in the left ventricular ejection fraction (LVEF) from 1 month after transplantation, whereas the control group showed no significant improvement (Figure S2). Furthermore, CMR showed that the iPS-CM group displayed a significantly greater LVEF at 3 months after transplantation (37.8% ± 2.3% vs. 28.3% ± 2.5%, $p = 0.019$) and significantly reduced left ventricular end-diastolic and systolic volumes compared to the pre-treatment ones (Figure 4A-4D). Analysis of MRI assessed in delayed enhanced images revealed that the infarct area in the iPS-CM group 3 months after implantation was significantly smaller than that in the control group. (22.7 ± 1.4 versus 17.6 ± 1.2 %, $p<0.01$, Figure 4E).

Hemodynamic parameters were also evaluated before transplantation and 3 months post-transplantation by left heart catheterization, which revealed that cardiac output was significantly higher in the iPS-CM group. Further, the left ventricular end diastolic pressure was significantly lower in the iPS-CM group than that in the control group (Figure 4F-M).

Telemetry was performed for 72 hours after transplantation (n=3, each group), revealing that lethal ventricular arrhythmias were not detected in either group.

In addition, we evaluated the global and regional cardiac function using CMR tissue tracking (Figure 5A). The iPS-CM group showed a significantly more improved global longitudinal strain (GLS) than the control group (ΔGLS; -1.9 ± 0.7 vs. 1.8 ± 0.9, p = 0.009, Figure 5B). As for the regional cardiac function, longitudinal strain in the border zones showed a significant improvement, whereas the infarct zone showed no significant improvement (Figure 5C-E).

iPS-CM transplantation promoted angiogenesis and inhibited fibrosis in border zone

We evaluated the pathological left ventricular (LV) remodeling 3 months after transplantation. Although all specimens had myocardial infarction in the antero-septal region, LV structure was better preserved in the iPS-CM group than in the control group (Figure 6A). The ratio of interstitial fibrosis at the border zone was significantly lower in the iPS-CM group than in the control group (12.6% ± 2.1% vs. 30.2% ± 5.8%, $p < 0.05$, Figure 6B). Furthermore, the cardiomyocyte size at the border zone was significantly smaller in the iPS-CM group than in the control group (iPS-CM group vs. control, 21.0 ± 1.7 μm versus 32.3 ± 1.3 μm, $p < 0.05$, Figure 6C). We also assessed angiogenesis at the border zone using CD31 and isolectin staining. Transplantation of cardiac tissue significantly promoted capillary density in the

border zone, compared with the control group (Figure 6D). Similarly, isolectin staining of the border zone revealed more structurally apparent microcapillaries in the iPS-CM group than in the control group (Figure 6E). Moreover, gene expression of proangiogenic cytokines in the border region 3 months after transplantation was evaluated using real-time polymerase chain reaction for vascular endothelial growth factor (VEGF), hepatocyte growth factor (HGF), basic fibroblast growth factor (b-FGF), stromal derived factor-1 (SDF-1), angiopoietin-1 (Ang-1), and angiopoietin-2 (Ang-2). The relative expression levels of all measured cytokines in the border zone of the iPS-CM group did not show significant differences between the two groups (Figure S3).

Transplantation of aligned cardiac tissue engraft with a partially preserved alignment of cardiomyocytes

We evaluated the engraftment of the transplanted tissue via immunofluorescent staining of human cTnT and *in situ* hybridization using a human-specific genomic probe (Figure 7A). A small number of human genome-positive nuclei were detected in the transplanted area 2 weeks after transplantation. The grafted cardiac tissue had a clear sarcomere structure revealed by using cTnT and α-actinin staining and remained partially aligned (Figure 7B). CD31 immunostaining revealed that the grafted tissue was well vascularized by the host vessels (Figure 7C). However, the expression of connexin 43 inside the transplanted tissue was still

weak and not localized compared to the host myocardium (Figure S4A), suggesting that it was structurally immature. Immunostaining for MLC2v and MLC2a in the engrafted tissue revealed that a large proportion of transplanted tissue was MLC2v-positive ventricular type myocardium, as seen prior to transplantation (Figure S4B). In addition, α-fetoprotein staining in engrafted tissues 2 weeks after transplantation revealed no endodermal tissue (Figure S4C). There was no obvious engraftment of the transplanted tissue 3 months after transplantation, probably due to the xenotransplantation effects.

Discussion

The main findings of the present study were the following: (1) high-purity cardiomyocytes could be robustly obtained using a protein-free, cost-effective, small-molecule-based protocol. (2) A simple and practical method to create large-scale aligned cardiac tissues was established, and the aligned cardiac tissue revealed enhanced contractile properties compared with the non-aligned cardiac tissue. (3) Transplantation of this cardiac tissue improved LV contractility in a porcine ischemic cardiomyopathy heart, and a limited number of cardiac tissues survived and demonstrated alignment in transplanted cardiomyocytes, 2 weeks after transplantation. (4) Transplantation of the aligned cardiac tissue enhanced angiogenesis and alleviated fibrosis in the peri-infarct area, resulting in left ventricular reverse remodeling.

The development of iPS cell differentiation into cardiomyocytes is an essential point for clinical application in terms of safety, cost, and a stable supply of cardiomyocytes. In recent years, various methods of cardiomyocyte differentiation from iPS cells with a high purity have been reported. However, these reports require the use of a large number of proteins, including costly growth factors, for cardiomyogenic differentiation, leading to cost and clinical safety issues[3,10]. Cardiomyocyte differentiation using small molecules in the present study may be a crucial step in the development of low-cost regenerative therapies using iPS cells [4–6,11]. The maturation cardiomyocytes in the present study were characterized by a relatively high number of mature ventricular cells with a morphologically developed sarcomere structure. However, it is controversial whether mature or immature cells are more potent in the restoration of cardiac function. When targeting cytokine-induced angiogenesis, transplantation of immature cardiomyocytes, which have been reported to release high levels of some angiogenesis-related cytokines, might have a better potential than transplantation of mature cardiomyocytes[12].

It is also important to discuss the underlining mechanisms in the improvement of cardiac function after transplantation, especially concerning cell maturation. The drawback of transplantation of immature cardiomyocytes is the possibility of arrhythmias due to electrical immaturity and tumorigenicity[13,14]. Considering the direct contractile augmentation by the

cardiac tissue graft, transplantation of mature cardiomyocytes, which may have powerful contractile force and developed sarcomeres, might have advantages compared to immature cell transplantation. Unfortunately, although it was difficult to achieve a perpetual engraftment of cardiac tissue in the present study, transplantation of mature cardiomyocytes may establish the primary aim of cardiomyogenesis using previous reported methods concerning enhanced engraftment via co-transplantation with mesenchymal stem cells or omentum[15–17]. In addition, regarding the subtype of transplanted cardiomyocytes, it is obvious that ventricular cardiomyocytes with more contractile proteins would be more advantageous for "Cardiomyogenesis"

Cardiomyocyte alignment of the transplanted tissue is also one of the key factors for "Cardiomyogenesis" therapy for heart failure. Adult cardiomyocytes have a sophisticated alignment *in vivo*, optimizing the contractile force in the same direction[18]. In patients with hypertrophic cardiomyopathy, a disarray of cardiomyocytes has been identified to be responsible for a deteriorated contractility[19]. Our data indicated that the contractile function of the aligned myocardial tissue might be greater than that of the non-aligned tissue. The reason why the aligned cardiac tissue was more powerful could be the stronger cell-cell adhesion in the aligned cardiac tissue, which promotes synchronization and anisotropic propagation as a whole cardiac tissue, leading to an augmented contractility. An enhanced structural maturity,

including the existence of a clear Z band, might also contribute to the augmented force[7]. Therefore, transplantation of the aligned cardiac tissue has a distinct advantage for future cell therapies with sufficient tissue engraftment.

As for the mechanism of improvement of cardiac function in the present study, regional cardiac function analysis using CMR tissue tracking revealed an improvement in the peri-infarct area, but not in the infarct area. Histology analysis also indicated the engraftment of the aligned cardiac tissue 2 weeks after transplantation, which was unclear at 3 months. These findings suggest that the possible mechanism of improved cardiac function may depend on angiogenesis via the paracrine effect with myocardial blood flow in the peri-infarct zone, rather than on the direct mechanical support provided by the transplanted cardiac tissue.

There were a few limitations to this study. Although we mainly focused on the electrophysiological and mechanical advantages of the aligned cardiac tissues, their potential benefits were not thoroughly achieved in *in vivo* experiments because of insufficient engraftment. Further studies, such as the development of the immune system and novel transplantation methods, are required to reveal these benefits *in vivo*.

In conclusion, large-scale cardiac tissue with aligned nanofiber scaffolds ameliorated the cardiac function in a porcine ischemic cardiomyopathy model as a proof of concept for clinical trials.

Financial Disclosure Statement

This work was supported by the Japan Society for the Promotion of Science (JSPS) Grants-in-Aid for Scientific Research (C) (19k12801) and Grants-in-Aid for Young Scientist (B) (18k16392). This research was partially supported by the Japan Agency for Medical Research and Development (AMED) Program.

Author contributions

K.S., Y.S., S.M., and L.L. conceived the project. K.S., Y.S., S.M., L.L., J.L., and T.K. designed the experiments. Y.S., S.M., and L.L. contributed to the acquisition of funding. All authors contributed to data analysis and interpretation. K.S., J.L., L.L, and S.M. wrote the manuscript.

Acknowledgments

We greatly appreciate Itsunari Minami and Mari Wakabayashi for their advice and experimental support on the differentiation of cardiomyocytes from iPS cells.

Figure Legends

Figure 1

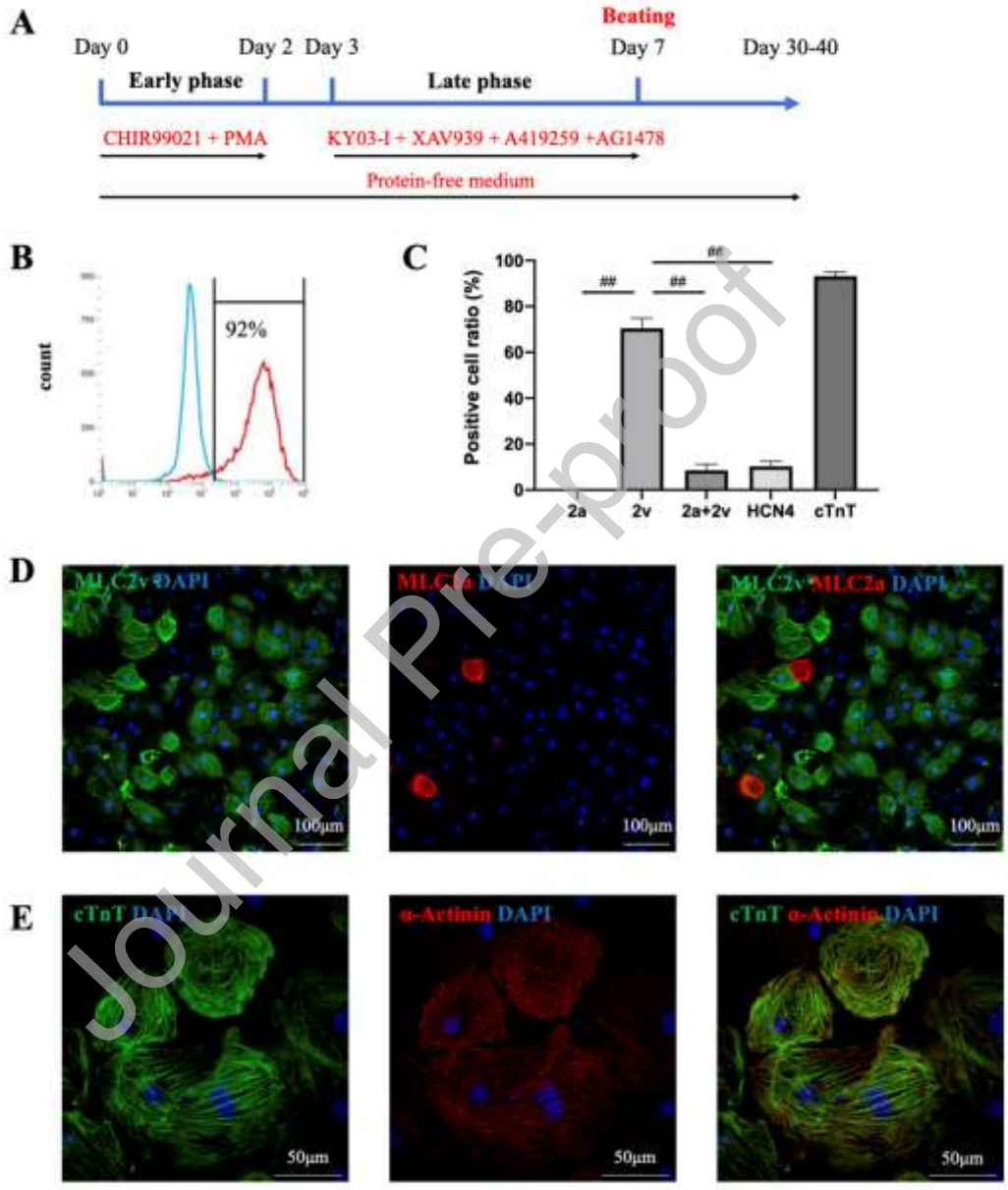

Figure 1: Characterization of human induced-pluripotent stem cells derived cardiomyocyte (hiPS-CMs) under protein-free conditions.

A: Schematic diagram of the protein-free differentiation method. In the early phase of differentiation (days 0 - 2), the pre-cultured hiPS-cell aggregates were cultured in protein-free medium containing a GSK3β inhibitor (2 μM CHIR99021) and a PKC activator (0.3 μM PMA). In the late phase (days 3 - 7), cells were cultured in medium with WNT inhibitors (3 μM KY03-I and 1 μM XAV939), an Src inhibitor (0.3 μM A419259), and an EGFR inhibitor (10 μM AG1478). Beating cardiac colonies usually emerged from days 7 to 9.

B: Representative flow cytometry data of cTnT-positive cells differentiated from hiPSCs (253G1) using the protein-free differentiation method.

C: Histograms of cardiac markers (MLC2v, MLC2a, HCN4, and cTnT) expressed in hiPS-CMs. Positive cell ratios were measured on day 30. The experiment was independently performed four times (n=4). ## $P<0.01$ by one-way ANOVA followed by Tukey's post-hoc test.

D: Immunostaining for MLC2v (green) and MLC2a (red) in hiPS-CMs (day 30).

E: Immunostaining for cTnT (green) and α-actinin (red) in hiPS-CMs (day 30).

Figure 2

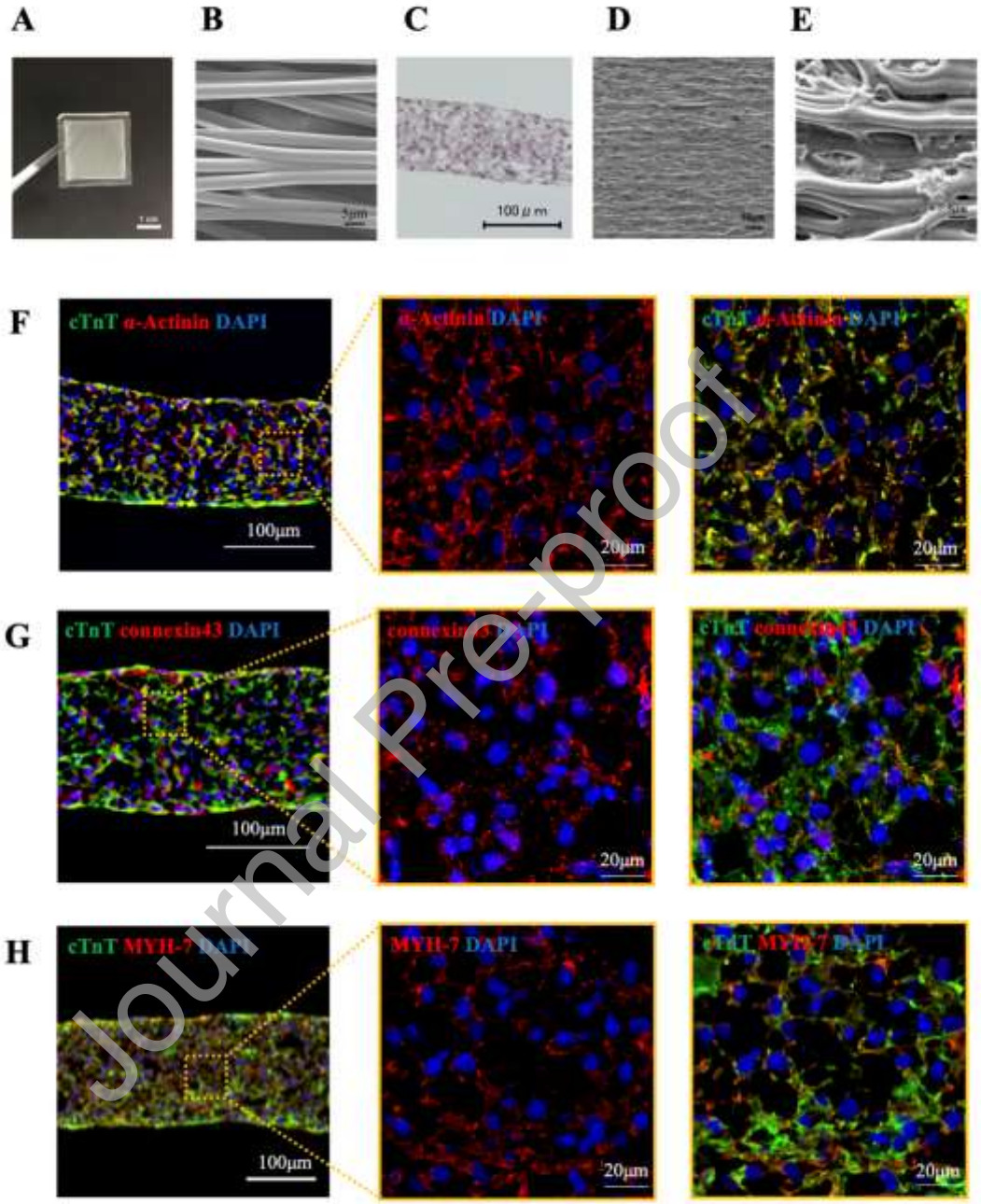

Figure 2: Fabrication of large aligned cardiac tissue using a nanofiber scaffold.

A: Macroscopic image of large sized aligned nanofiber (2.5 cm × 2.5 cm).

B: Scanning electron microscopy (SEM) image of the aligned nanofibers.

C: Hematoxylin and eosin staining of the aligned cardiac tissue.

D-E: SEM image of the aligned cardiac tissue.

F-H: Immunostaining image of the aligned cardiac tissue for (F) cTnT (green) and α-actinin (red). (G) cTnT (green) and connexin 43 (red), (H) cTnT (green), and MYH7 (red).

Figure 3

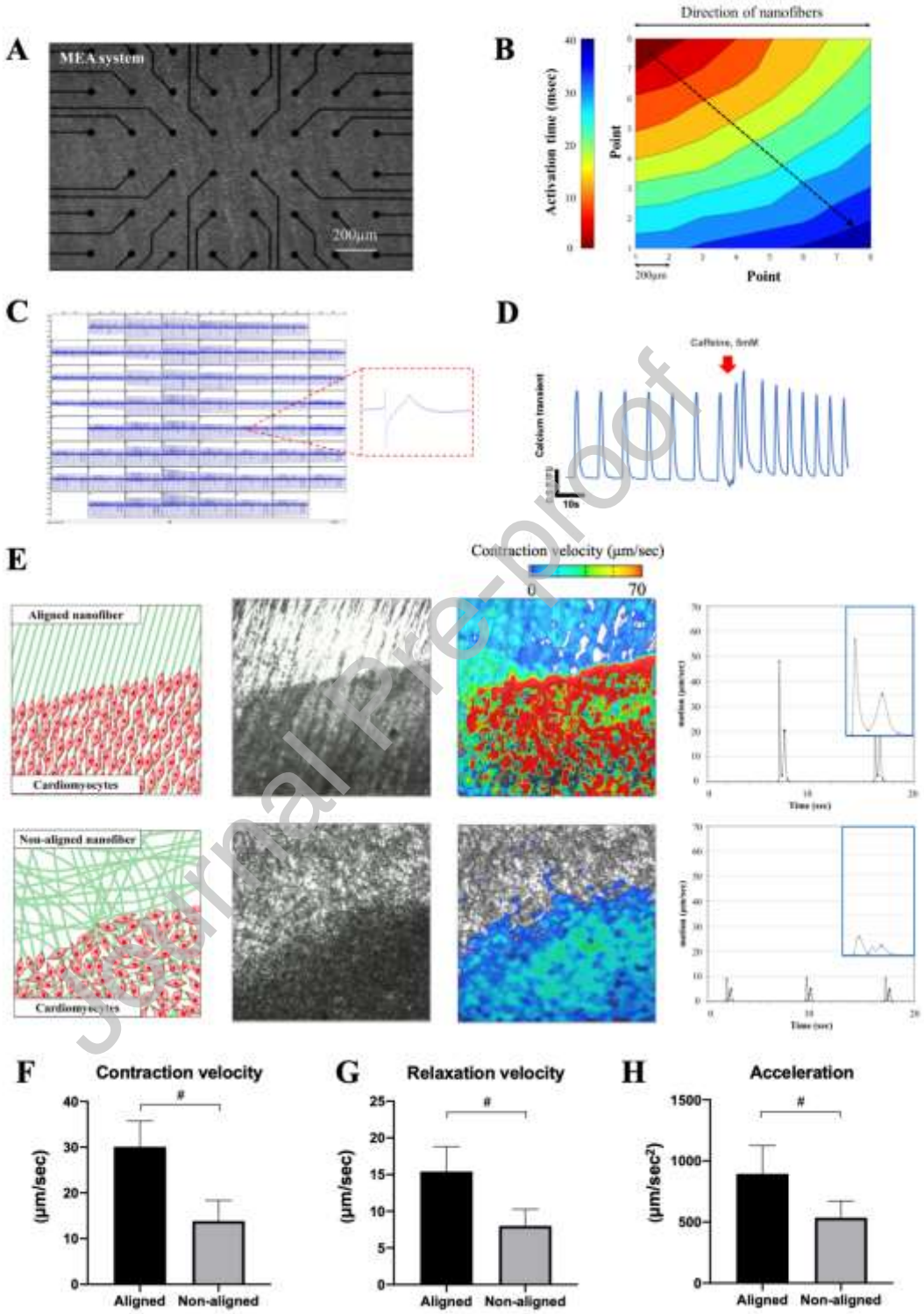

Figure 3: Functional analysis of the aligned cardiac tissue.

A: Microscopic representation of the aligned cardiac tissue on top of a MEA.

B: Activation map showing the propagation of stimulated contractility.

C: Representative homogeneous electrogram recording from a large scale aligned cardiac tissue (n=3).

D: Calcium transient of aligned cardiac tissue (n=3). Aligned cardiac tissue responded to the addition of 5mM caffeine (red arrow), a significantly higher peak intensity was observed.

E: Representative velocity image of the aligned cardiac tissue (upper panel) and non-aligned cardiac tissue (lower panel) using a motion analysis system (far left panel: schematic diagram; second panel: without color; third panel: representative velocity images with color; far right: plot of a motion waveform showing contraction and relaxation velocity peaks). Red and blue represent high and low velocities, respectively.

F-H: Contractile properties of the aligned cardiac tissue and non-aligned cardiac tissue (n = 6). (F) Contraction velocity, (G) relaxation velocity, and (H) acceleration. ## $P<0.05$ by Student's *t*-test

Figure 4

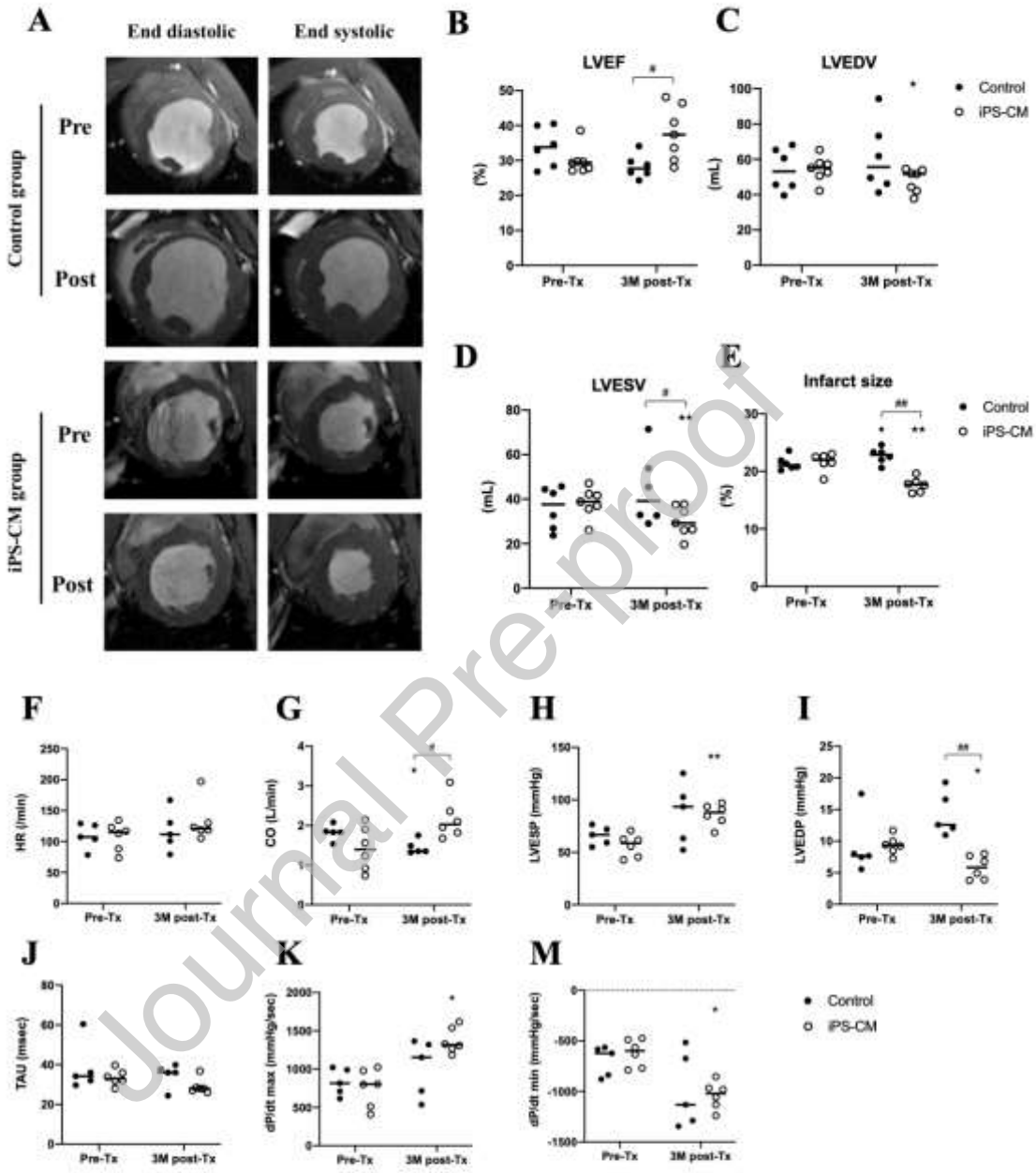

Figure 4: Aligned cardiac tissue transplantation improves cardiac function, as shown by cardiac magnetic resonance images (CMR).

A-E: (A) Magnetic resonance images (MRI) at end diastolic and end systolic phase (upper panel: before transplantation, lower panel:3 months after transplantation) were obtained and used to measure (B) left ventricular ejection fractions (LVEF), (C) left ventricular end-diastolic volume (LVEDV), (D) left ventricular end-diastolic volumes (LVESV), and (E) infarct sizes.

F-M: Hemodynamic parameters were evaluated before transplantation (pre-Tx) and 3 months post-transplantation (3M-Tx) by left heart catheterization. (F) heart rate (HR), (G) cardiac output (CO), (H) left ventricular end systolic pressure (LVESP), (I) left ventricular end diastolic pressure (LVEDP), (J) TAU, (K) dP/dt max, (M) dP/dt min, ★ $p<0.05$ versus Pre-Tx, ★★ $p<0.01$ versus Pre-Tx by paired t-test, # $P<0.05$ between control and iPS-CM, ## $P<0.01$ between control and iPS-CM by Student's *t*-test

Figure 5

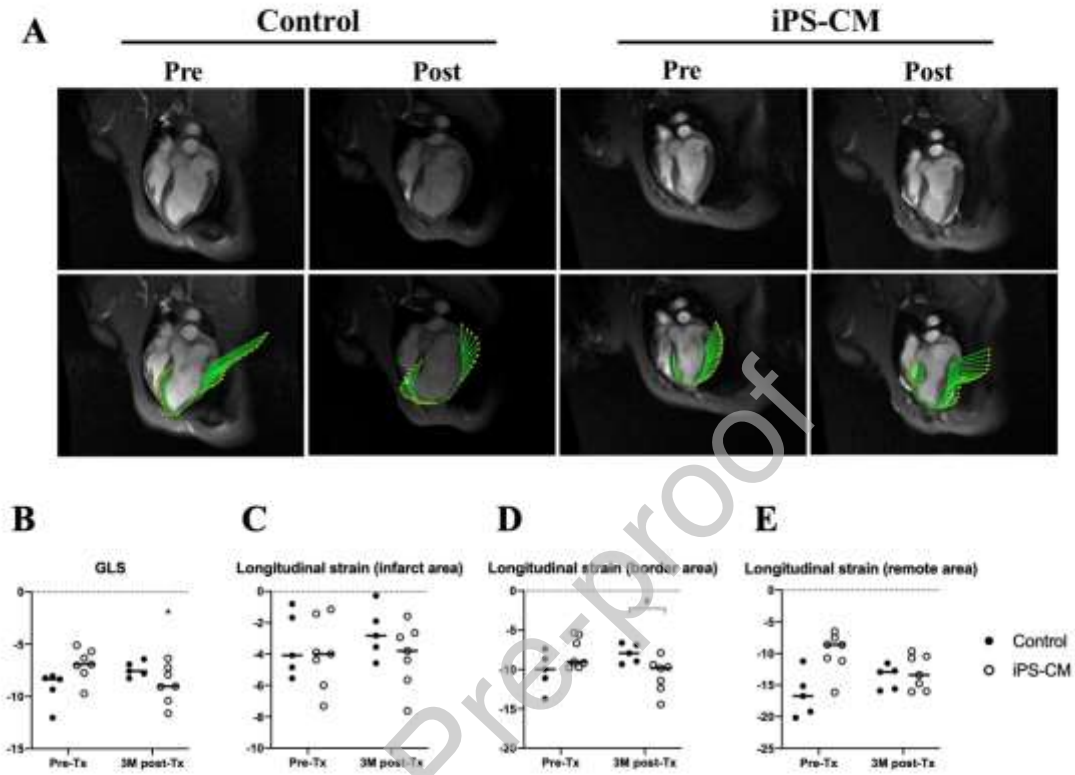

Figure 5: Improvement of regional cardiac function assessed by feature-tracking analysis with cardiac magnetic resonance imaging (CMR)

A: Representative images of endocardial systolic wall motion at apical 4 chamber view. The length of the velocity vector represents the relative speed at any given time.

B-E: Feature-tracking analysis with CMR before transplantation (Pre-Tx) and at 3 months post-transplantation (3M-Tx) by left heart catheterization. Global longitudinal strain (GLS) (B), longitudinal strain in infarct area (C), longitudinal strain in border area (D), longitudinal strain in remote area (E), ★ $p<0.05$ versus Pre-Tx by paired t-test, # $P<0.05$ between control and iPS-CM by Student's *t*-test.

Figure 6

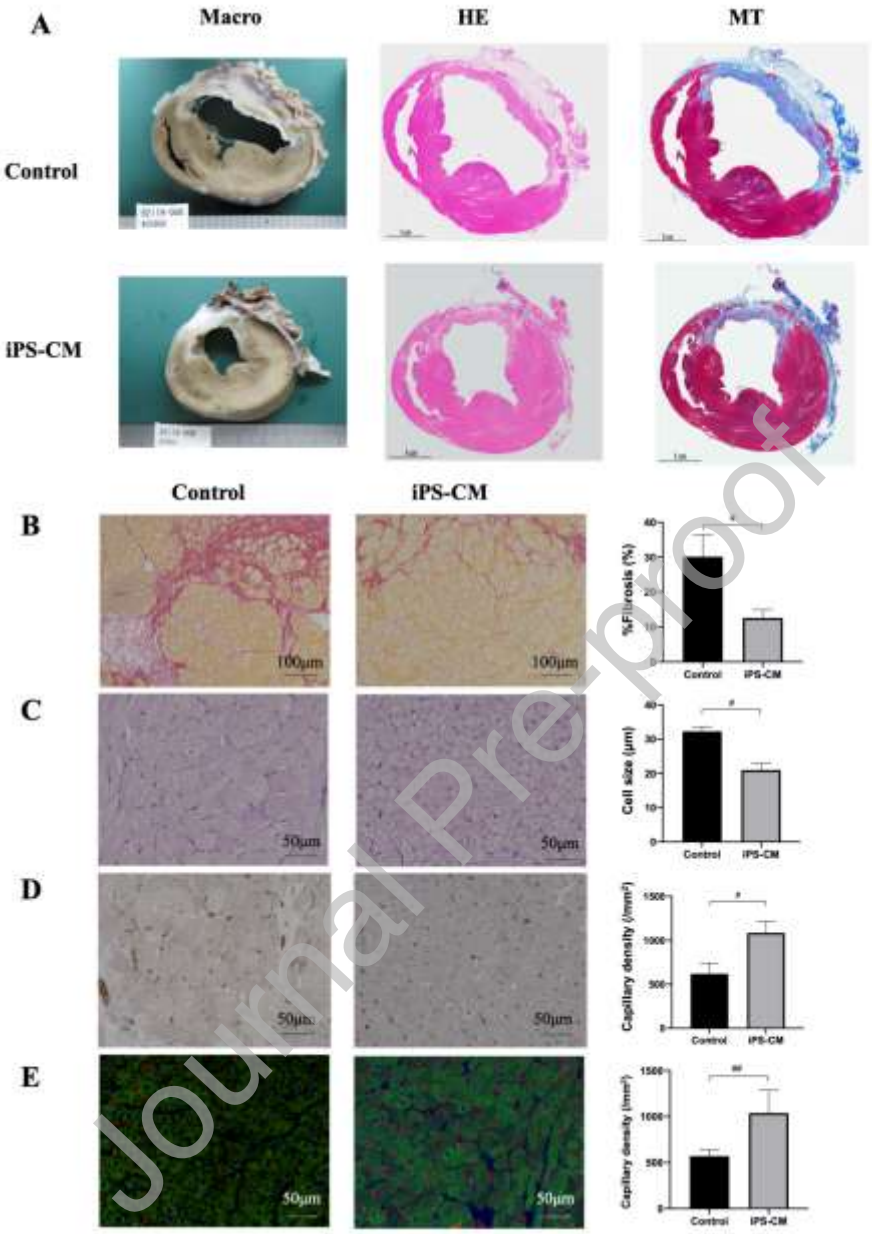

Figure 6: Histology of the extracted heart, 3 months after transplantation.

A: Representative image of the whole extracted heart at the left ventricular papillary muscle level (left panel: macro; middle panel: HE, hematoxylin eosin staining; right panel: MT, mason trichrome staining).

B–E: Representative microscopic images and quantitative data of border area in the extracted heart (n=6 for each group, B: Sirius red staining, fibrosis; C: Periodic acid-Schiff staining, cardiomyocyte size; D: CD-31 staining, capillary density, E: Isolectin staining [Green: cTnT, Red: isolectin]), # P<0.05 between control and iPS-CM, ## P<0.01 between control and iPS-CM by Student's *t*-test.

Figure 7

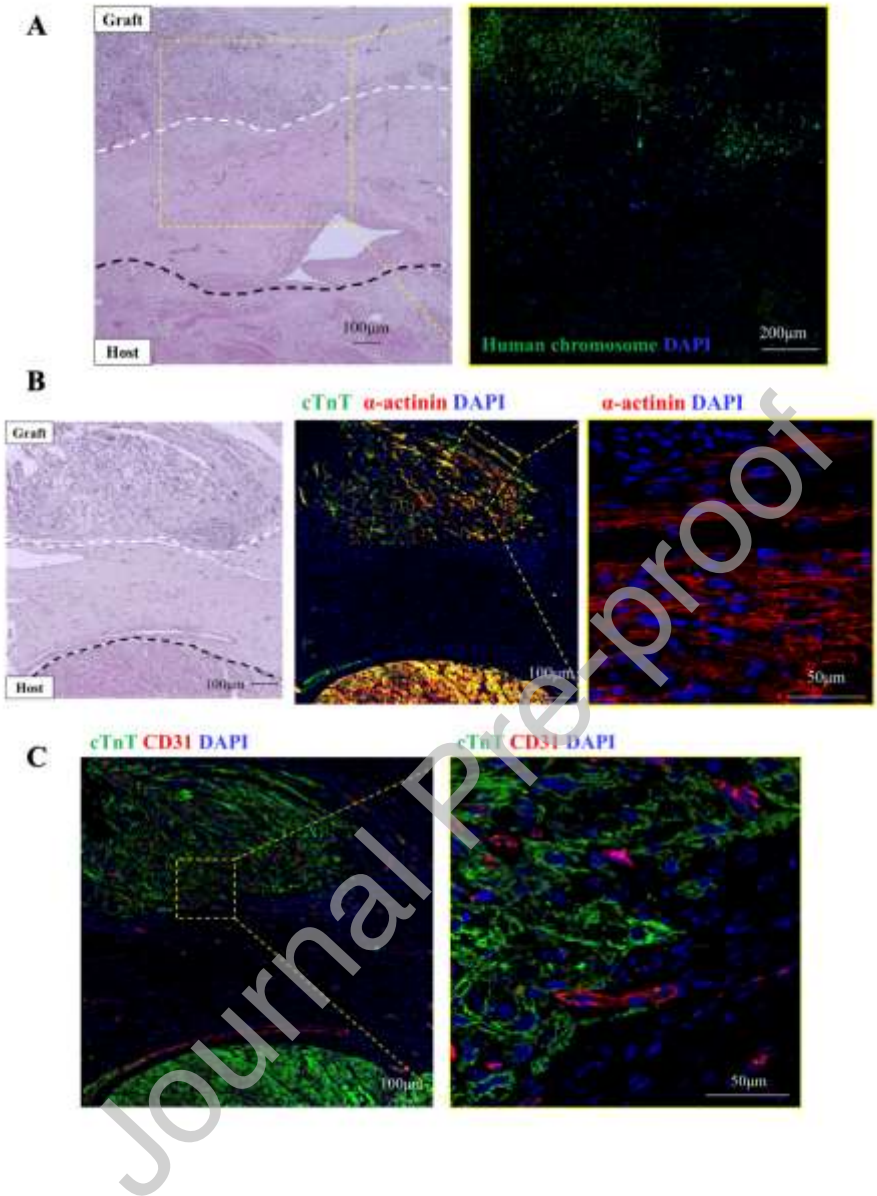

Figure 7: Aligned cardiac tissue engraftment, 2 weeks after transplantation.

A: Transplanted tissue engraftment was identified 2 weeks after transplantation (left panel: HE staining of transplanted area; Right panel: species-specific fluorescent *in situ* hybridization using human specific probe (green)).

B: Transplanted tissue showed well-organized sarcomeric structures (left panel: hematoxylin eosin staining; middle panel: immunostaining of human cTnT (green) and α-actinin (red)). A representative sarcomeric structure with tissue alignment is shown in the inset (right panel).

C: Immunostaining of cTnT (green) and CD31 (red) illustrating that the transplanted tissue was well vascularized.

References

1. Kawamura M, Miyagawa S, Miki K, et al. Feasibility, Safety, and Therapeutic Efficacy of Human Induced Pluripotent Stem Cell-Derived Cardiomyocyte Sheets in a Porcine Ischemic Cardiomyopathy Model. *Circulation*. 2012;126(11_suppl_1):S29-S37.

2. Ishida M, Miyagawa S, Saito A, et al. Transplantation of Human-induced Pluripotent Stem Cell-derived Cardiomyocytes Is Superior to Somatic Stem Cell Therapy for Restoring Cardiac Function and Oxygen Consumption in a Porcine Model of Myocardial Infarction: *Transplantation*. 2019;103(2):291-298.

3. Sasano Y, Fukumoto K, Tsukamoto Y, Akagi T, Akashi M. Construction of 3D cardiac tissue with synchronous powerful beating using human cardiomyocytes from human iPS cells prepared by a convenient differentiation method. *Journal of Bioscience and Bioengineering*. 2020;129(6):749-755.

4. Lian X, Hsiao C, Wilson G, et al. Cozzarelli Prize Winner: Robust cardiomyocyte differentiation from human pluripotent stem cells via temporal modulation of canonical Wnt signaling. *Proceedings of the National Academy of Sciences*. 2012;109(27):E1848-E1857.

5. Burridge PW, Matsa E, Shukla P, et al. Chemically defined generation of human cardiomyocytes. *Nat Methods*. 2014;11(8):855-860.

6. Minami I, Yamada K, Otsuji TG, et al. A Small Molecule that Promotes Cardiac Differentiation of Human Pluripotent Stem Cells under Defined, Cytokine- and Xeno-free Conditions. *Cell Reports*. 2012;2(5):1448-1460.

7. Li J, Minami I, Shiozaki M, et al. Human Pluripotent Stem Cell-Derived Cardiac Tissue-like Constructs for Repairing the Infarcted Myocardium. *Stem Cell Reports*. 2017;9(5):1546-1559.

8. Khan M, Xu Y, Hua S, et al. Evaluation of Changes in Morphology and Function of Human Induced Pluripotent Stem Cell Derived Cardiomyocytes (HiPSC-CMs) Cultured on an Aligned-Nanofiber Cardiac Patch. Pesce M, ed. *PLoS ONE*. 2015;10(5):e0126338.

9. Yajima S, Miyagawa S, Fukushima S, et al. A prostacyclin agonist and an omental flap increased myocardial blood flow in a porcine chronic ischemia model. *The Journal of Thoracic and Cardiovascular Surgery*. 2018;156(1):229-241.e14.

10. Kadari A, Mekala S, Wagner N, et al. Robust Generation of Cardiomyocytes from Human iPS Cells Requires Precise Modulation of BMP and WNT Signaling. *Stem Cell Rev and Rep*. 2015;11(4):560-569.

11. Jiang Y, Lian XL. Heart regeneration with human pluripotent stem cells: Prospects and challenges. *Bioactive Materials*. 2020;5(1):74-81.

12. Yan L, Guo H, Hu B, et al. Epigenomic Landscape of Human Fetal Brain, Heart, and Liver. *J Biol Chem*. 2016;291(9):4386-4398.

13. Chong JJH, Yang X, Don CW, et al. Human embryonic-stem-cell-derived cardiomyocytes regenerate non-human primate hearts. *Nature*. 2014;510(7504):273-277.

14. Shiba Y, Gomibuchi T, Seto T, et al. Allogeneic transplantation of iPS cell-derived cardiomyocytes regenerates primate hearts. *Nature*. 2016;538(7625):388-391.

15. Kawamura M, Miyagawa S, Fukushima S, et al. Enhanced Survival of Transplanted Human Induced Pluripotent Stem Cell-Derived Cardiomyocytes by the Combination of

Cell Sheets With the Pedicled Omental Flap Technique in a Porcine Heart. *Circulation*. 2013;128(11_suppl_1):S87-S94.

16. Kawamura M, Miyagawa S, Fukushima S, et al. Enhanced Therapeutic Effects of Human iPS Cell Derived-Cardiomyocyte by Combined Cell-Sheets with Omental Flap Technique in Porcine Ischemic Cardiomyopathy Model. *Sci Rep*. 2017;7(1):8824.

17. Yoshida S, Miyagawa S, Fukushima S, et al. Maturation of Human Induced Pluripotent Stem Cell-Derived Cardiomyocytes by Soluble Factors from Human Mesenchymal Stem Cells. *Molecular Therapy*. 2018;26(11):2681-2695.

18. Siedner S, Kruger M, Schroeter M, et al. Developmental changes in contractility and sarcomeric proteins from the early embryonic to the adult stage in the mouse heart. *The Journal of Physiology*. 2003;548(2):493-505.

19. Marian AJ, Braunwald E. Hypertrophic Cardiomyopathy: Genetics, Pathogenesis, Clinical Manifestations, Diagnosis, and Therapy. *Circ Res*. 2017;121(7):749-770.